

## Preparation of a Au SERS substrate and its application in the in-situ Raman spectroelectrochemistry study of $\text{Li}_2\text{CO}_3\text{-K}_2\text{CO}_3$ molten salt

Jiangyu Yu<sup>1</sup>, Chengyuan Liu<sup>1</sup>, Xianwei Hu<sup>1,\*</sup>, Tian Yuan<sup>1</sup>, Yifan Zhang<sup>1</sup>, Zhaowen Wang<sup>1</sup>, Wuren Ji<sup>2,\*</sup>

<sup>1</sup> School of Metallurgy, Northeastern University, Shenyang 110819, China

<sup>2</sup> Northwest Research Institute of Mining and Metallurgy, Baiyin 730900, China

\*E-mail: [huxw@smm.neu.edu.cn](mailto:huxw@smm.neu.edu.cn), [tomcat3164@163.com](mailto:tomcat3164@163.com)

Received: 30 July 2021 / Accepted: 8 September 2021 / Published: 10 October 2021

---

Molten carbonate is often used as a medium for the decomposition of carbon dioxide to produce carbon and oxygen. In-situ Raman spectroelectrochemistry is an effective means to study species changes and the electrochemical reaction mechanism at the electrode-electrolyte interface. In this paper, a Au surface-enhanced Raman spectroscopy (SERS) substrate was prepared by an electrochemical oxidation-reduction cycle (ORC) process, and the reaction mechanism and intermediate species on this kind of Au SERS electrode in a  $\text{Li}_2\text{CO}_3\text{-K}_2\text{CO}_3$  molten salt were studied. The prepared Au SERS substrate has a SERS factor of  $1.37 \times 10^4$ , and it presents excellent uniformity and long-term stability. Although the SERS effect of the Au substrate gradually weakens as the temperature increases, it maintains an acceptable SERS factor of  $8.76 \times 10^2$  after a high-temperature treatment at 873 K. The cyclic voltammogram result shows that carbon reduction preferentially occurs on an Au electrode during the cathodic electrochemical process in  $\text{Li}_2\text{CO}_3\text{-K}_2\text{CO}_3$  molten salt. In-situ Raman spectroscopy confirms the existence of the intermediate peroxide ion ( $\text{O}_2^{2-}$ ) during the electrochemical reduction process.

---

**Keywords:** In-situ Raman spectroscopy; SERS; Carbonate molten salt; Peroxide ion

### 1. INTRODUCTION

Molten carbonate salts have received extensive attention because of their applications in high-temperature catalysis, fuel cells, thermal energy storage and carbon dioxide recovery [1-5]. The preparation of carbon and oxygen by the electrolysis of  $\text{CO}_2$  in molten carbonate salts is an effective process to realize the rational utilization of  $\text{CO}_2$ . Alkali metal carbonate is considered an ideal medium

in this process [6-10]. Thus, knowledge of the electrochemical behavior and internal structure of carbonate molten salts is very important.

Appleby *et al.* studied the electrochemical reaction of oxygen and carbonate ions in molten carbonate in an atmosphere of oxygen and carbon dioxide by steady-state and cyclic voltammetric electrochemical technologies [11-13]. They proposed three possible reaction pathways containing active peroxide ion ( $O_2^{2-}$ ), superoxide ion ( $O^{2-}$ ), and peroxy carbonate ion ( $CO_4^{2-}$ ) intermediates. In addition, the neutralization of the  $O^{2-}$  ion by  $CO_2$  was considered as the rate controlling step of the entire porous electrode reaction in alkali carbonate melts. Vogel *et al.* studied the solubility of oxygen in  $Li_2CO_3$ - $K_2CO_3$  (molar ratio of 62:38) molten salt using a rotating electrode, and found that the main oxygen-containing species in the molten salt is superoxide ions [14]. Cassir *et al.* studied the electrochemical processes and thermodynamics of oxygen reduction in alkali metal carbonate systems at different temperatures through cyclic voltammetry and rotating potential scanning techniques [15-16]. The results showed that peroxide ions can only exist stably in basic systems, and superoxide ions cannot exist in Li-containing carbonates but can stably exist in Na-K carbonates. In addition,  $CO_2$  participated in the rate-determining reduction of superoxide and peroxide ions. Van *et al.* measured the cyclic voltammetry curves recorded on a carbon electrode in molten Li-Na-K carbonates at the eutectic composition (43.5:31.5:25 in molar percentage) [17]. Peroxide ions adsorbed on the electrode during carbon electrodeposition, and could only stably exist on the carbon deposit. They also found that the concentration of peroxide ions on the electrode surface increased as the potential became more negative, resulting in a decrease in the electrode effective area. A similar result was also reported by Borucka [18].

In-situ Raman spectroelectrochemistry can provide changes in complex species on/near the electrode surface, which contributes to deeply studying the electrochemical reaction mechanism on the electrode [19-23]. Raman spectroscopy shows unique advantages in the research on melt structures and high-temperature chemical reactions [24-27]. Itoh *et al.* studied the cyclic voltammetry behavior of molten  $Li_2CO_3$ - $K_2CO_3$  and  $Li_2CO_3$  systems on a gold electrode, and thought that peroxide ions ( $O_2^{2-}$ ) and superoxide ions ( $O^{2-}$ ) were generated during the electrochemical reduction of oxygen, while peroxide ions could only exist in the  $Li_2CO_3$  system [28-29].

Conventional Raman spectroscopy technology is limited in its application in high-temperature molten salts because the Raman scattering signal was too weak to detect the required surface or interface. Surface-enhanced Raman scattering (SERS) technology is usually used to increase the Raman scattering signal, which can significantly enhance the Raman scattering signal of species adsorbed on certain metal surfaces by several orders of magnitude [30-31]. SERS has been widely used for the in-situ study of various solid-liquid, solid-gas, and solid-solid interface systems at the molecular level to characterize the structure and process of surfaces (interfaces), especially identifying the weak Raman signal of intermediate species in electrochemical reactions [32-33]. To achieve an in-depth understanding of the electrochemical mechanism of carbonate molten salt and expand the application of SERS technology in high-temperature molten salts, a Au SERS substrate was prepared by an electrochemical oxidation-reduction cycle (ORC) process [34] in this paper, and the electrochemical reaction mechanism and intermediate species on the polished and Au SERS electrodes were studied in  $Li_2CO_3$ - $K_2CO_3$  molten salt by in-situ Raman spectroelectrochemistry.

## 2. EXPERIMENTAL

The Au SERS substrate was prepared by the ORC process in  $0.1 \text{ mol}\cdot\text{L}^{-1}$  KCl aqueous solution. A polished Au sheet and a platinum sheet were used as the working and counter electrodes respectively, and the reference electrode was a saturated calomel electrode. The electrochemical treatment process of the polished Au substrate is shown in Figure 1.

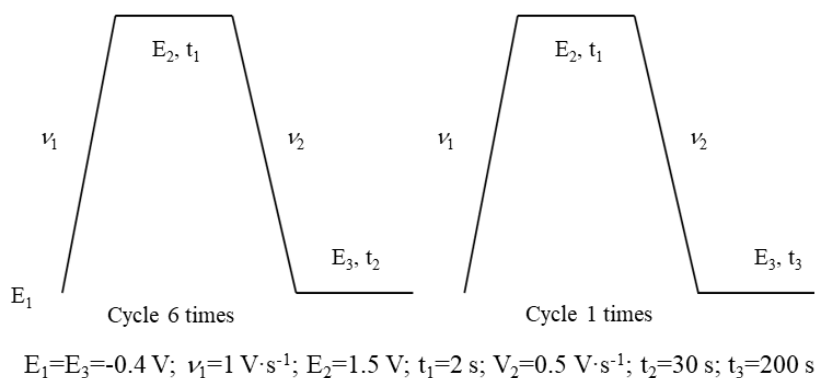


**Figure 1.** The diagram of the ORC process for Au SERS substrate preparation

Rhodamine 6G (R6G) was used as the probe molecule to test the SERS effect of the Au SERS substrate. The substrate was immersed in a  $10^{-4} \text{ mol}\cdot\text{L}^{-1}$  aqueous solution of R6G for more than 2 hours and then rinsed with deionized water to remove the adsorbed chemical. The Raman spectra were recorded via a Raman spectrometer (Horiba Jobin Yvon LabRAM HR 800).

Cyclic voltammogram measurements were carried out in the  $\text{Li}_2\text{CO}_3\text{-K}_2\text{CO}_3$  molten salt (68:32 in molar percentage) to study the reaction mechanism on the electrode surface during the cathodic electrochemical process. All experiments were processed with a three-electrode assembly. An Au wire was used as an inert working electrode, and the active electrode surface area was calculated by the immersion depth of the electrode in the molten salt. A platinum wire and graphite rod were used as the quasi-reference electrode and counter electrode, respectively. All electrodes were polished thoroughly with emery paper and then cleaned with ethanol before use. For the in-situ Raman spectroelectrochemistry study, the prepared Au SERS substrate was used as the working electrode. The excitation light of an  $\text{Ar}^+$  laser with a wavelength of 488.2 nm was focused on the interface between the electrolyte and electrode through a  $50\times 0.50$  objective (Olympus). The power of the laser beam was controlled at approximately 17 mW. The spectrum acquisition time was set as 15 s with 2 accumulations.

## 3. RESULTS AND DISCUSSION

The morphologies of the prepared Au SERS substrate are shown in Figure 2. A large number of hill-like and ravine-like structures exist on the Au SERS substrate. These rough and uneven surfaces contribute to the SERS enhancement effect.

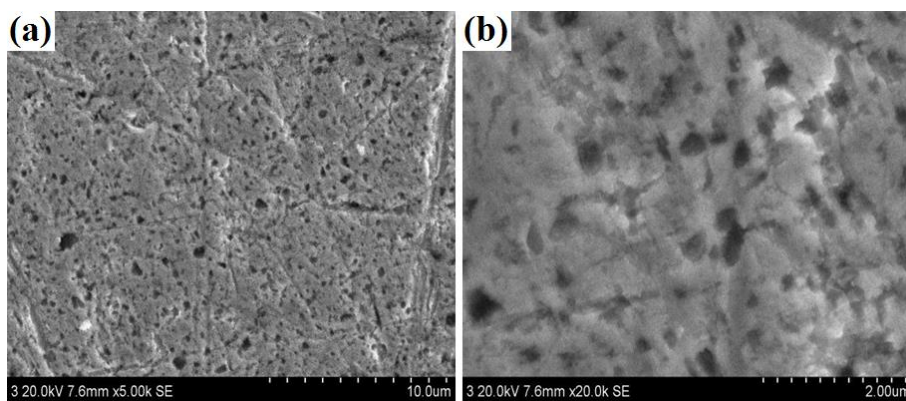


**Figure 2.** Morphologies of the prepared SERS Au substrate: (a) scale bar: 10 μm; (b) scale bar: 2 μm

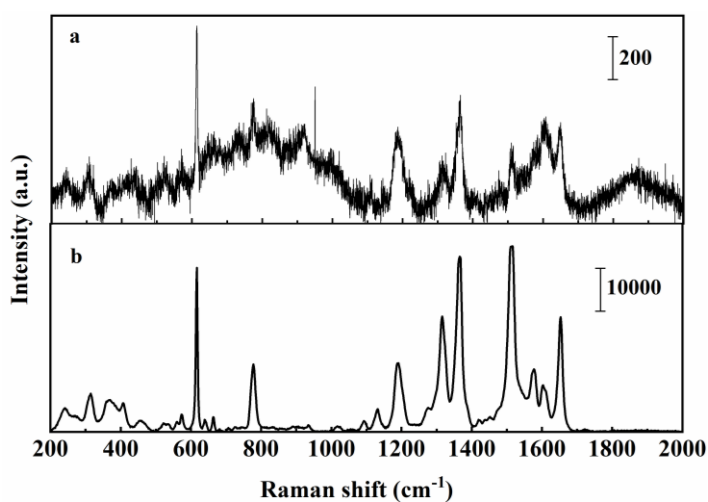


**Figure 3.** Raman spectra of (a) R6G aqueous solution ( $10^{-4} \text{ mol}\cdot\text{L}^{-1}$ ) and (b) R6G aqueous solution ( $10^{-4} \text{ mol}\cdot\text{L}^{-1}$ ) adsorbed on the Au SERS substrate

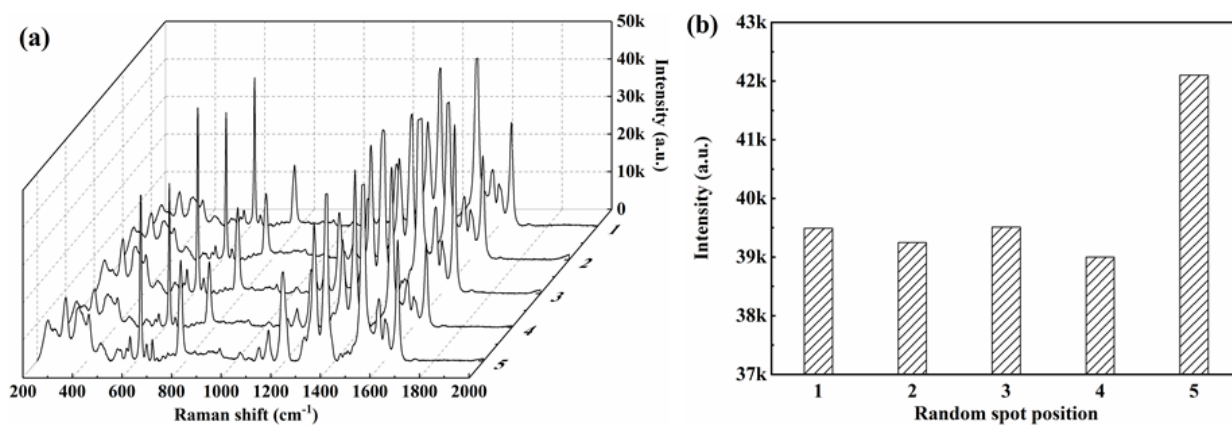


**Figure 4.** (a) Raman spectra of R6G aqueous solution acquired for five various points on the Au SERS substrate and (b) the corresponding Raman band intensity

Figure 3 shows the Raman spectra of R6G on the Au substrate. It is clearly observed that the prepared Au substrate exhibits an excellent SERS effect. The measured SERS intensities were compared with the intensity of normal Raman scattering to estimate the magnitude of the enhancement factor ( $EF$ ) using Equations (1)-(3) [35]:

$$EF = \frac{I_{\text{surf}}}{I_{\text{bulk}}} \times \frac{N_{\text{bulk}}}{N_{\text{surf}}} \quad 1)$$

$$N_{\text{bulk}} = Ahc_{\text{bulk}}N_A \quad 2)$$

$$N_{\text{surf}} = \frac{c_{\text{surf}}vN_A A}{\pi r^2} \quad 3)$$

where  $I_{\text{surf}}$  is the measured SERS intensity for R6G molecules absorbed on the SERS substrate, cps;  $I_{\text{bulk}}$  is the measured intensity of normal Raman scattering from R6G bulk solution, cps;  $N_{\text{bulk}}$  and  $N_{\text{surf}}$  are the numbers of R6G molecules in the bulk solution effectively illuminated by the laser beam and absorbed on the SERS substrate, respectively;  $A$  is the laser focal area,  $\text{cm}^2$ ;  $c_{\text{bulk}}$  is the concentration of R6G bulk solution,  $10^{-4} \text{ mol}\cdot\text{L}^{-1}$ ;  $N_A$  is the Avogadro constant,  $6.02 \times 10^{23} \text{ mol}^{-1}$ ;  $h$  is the confocal depth,  $1.3 \times 10^{-5} \text{ cm}$ ;  $c_{\text{surf}}$  and  $v$  are the concentration ( $10^{-4} \text{ mol}\cdot\text{L}^{-1}$ ) and volume ( $10^{-5} \text{ L}$ ) of R6G solution used for SERS detection; and  $r$  is the radius of  $10^{-5} \text{ L}$  R6G solution formed on the SERS substrate,  $0.35 \text{ cm}$ . Among them,  $I_{\text{SERS}}$  and  $I_{\text{norm}}$  were measured at  $1366 \text{ cm}^{-1}$ . The values of  $I_{\text{bulk}}$  and  $I_{\text{surf}}$  were measured to be 510 and  $6.98 \times 10^5$  cps, respectively. The value of the enhancement factor calculated for the prepared Au SERS substrate is  $1.37 \times 10^4$ .

The uniformity of the Au SERS substrate was further investigated by measuring the Raman enhancement effect of five various points on the Au SERS substrate. The center of the substrate and four right angles were used as the detection points, and the distances from the selected points at the four right angles to the center were equal. All the Raman spectra are shown in Figure 4(a). The intensities of the band at  $616.92 \text{ cm}^{-1}$  of the five Raman spectra are in the range of 39000 and 42000 (Figure 4(b)), which shows good reproducibility. The relative standard deviation (RSD) was used to evaluate the uniformity of the Au SERS substrate. The value of RSD is calculated to be 3.2% by Equation (4), indicating good uniformity.

$$RSD = \frac{\sqrt{\frac{\sum_{i=1}^n (I_i - \bar{I})^2}{n-1}}}{\bar{I}} \times 100\% \quad 4)$$

where  $I_i$  ( $i = 1, 2, 3, 4, 5$ ) and  $\bar{I}$  are the intensity and the average of the five Raman spectra for the band at  $616.92 \text{ cm}^{-1}$ , respectively;  $n$  is the number of collected spectra,  $n = 5$ .

A new Au SERS substrate was prepared to determine the stability of the SERS effect. The Raman spectrum of rhodamine 6G aqueous solution on the freshly prepared Au SERS substrate was first measured (spectrum (a) in Figure 5). Then the Raman spectrum of rhodamine 6G aqueous solution on the substrate stored in a dark and dry container for 30 days was obtained (spectrum (b) in Figure 5). The enhancement factors of the above Au SERS substrates with two various states were calculated based on the intensity of the band at  $618.04 \text{ cm}^{-1}$ . The enhancement factor of the Au SERS substrate stored for 30 days is only reduced by 18.2% compared with that of the fresh Au SERS substrate. It

shows the good long-term stability of the Au SERS substrate, which is attributed to the inactive property of the Au material and suitable storage conditions.

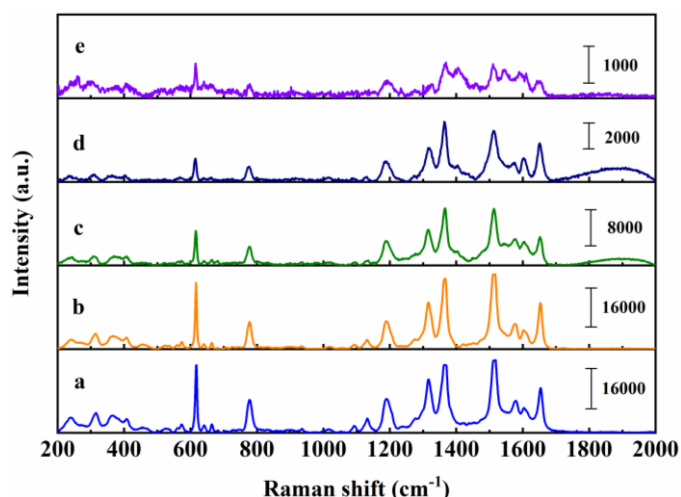


**Figure 5.** Raman spectra of R6G aqueous solution acquired from (a) freshly and (b) stored for thirty days Au SERS substrate; Au SERS substrate after heat-treatment at (c) 473 K, (d) 673 K, and (e) 873 K

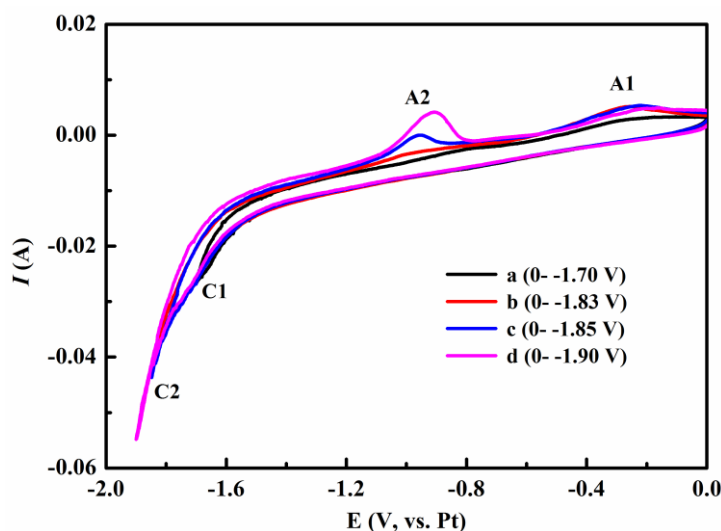


**Figure 6.** Cyclic voltammogram curves on the polished Au electrode in  $\text{LiCO}_3\text{-KCO}_3$  molten salt with a scan rate of  $20 \text{ mV}\cdot\text{s}^{-1}$  at 873 K (The indigo curve: 0--1.70 V (vs. Pt); the red curve: 0--1.83 V (vs. Pt); the blue curve: 0--1.85 V (vs. Pt); the purple line: 0--1.90 V (vs. Pt))

Furthermore, the effect of temperature on the Raman enhancement effect of the Au substrate was investigated, and the Raman spectra of rhodamine 6G aqueous solution on the Au SERS substrate after heat treatment at various temperatures (473, 673, and 873 K) are shown in Figure 5(c), (d), and (e). As observed from spectra (c), (d), and (e), the SERS effect of the Au substrate gradually weakens

as the heating temperature increases. After high-temperature treatment at 873 K, the enhancement factor of the Au SERS substrate maintained at  $8.76 \times 10^2$ , indicating that the Au substrate after heat treatment still presents an acceptable SERS effect. It is thus thought that the Au SERS substrate prepared by the ORC process has potential applications in research on in situ Raman spectroscopy in high-temperature molten salts.

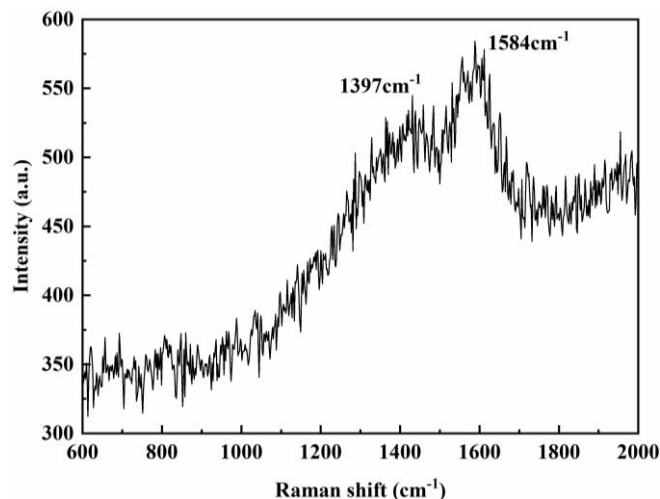


**Figure 7.** Raman spectrum of the deposit obtained from  $\text{Li}_2\text{CO}_3\text{-K}_2\text{CO}_3$  melt at  $-1.8$  V (vs. Pt) and 873 K

Figure 6 presents the cyclic voltammogram curves obtained on a polished Au electrode in  $\text{Li}_2\text{CO}_3\text{-K}_2\text{CO}_3$  molten salt at 873 K with a scan rate of  $20 \text{ mV}\cdot\text{s}^{-1}$ . Curve a shows only one reduction wave C1 and a small oxidation peak A1, and the peak current increases as the cathodic reversing potential moves to a negative value of  $-1.83$  V (curve b). A new reduction wave C2 and corresponding oxidation peak A2 occurred in the cyclic voltammogram curves (c and d) when the reversing potential was set as more negative values of  $-1.85$  V and  $-1.90$  V. Waves C1 and C2 are attributed to the reduction of carbon and lithium metal, respectively, and were also observed in previous reports of alkali metal carbonate [36]. The reduction process can be described as follows:



To further confirm the reduction reaction in wave C1, electrodeposition on a Au substrate was carried out in  $\text{Li}_2\text{CO}_3\text{-K}_2\text{CO}_3$  molten salt at  $-1.80$  V for 15 min. The Raman spectrum of the deposit is shown in Figure 7. Two typical bands appearing at  $1397$  and  $1584 \text{ cm}^{-1}$  were assigned to the D-band and G-band of carbon, respectively. Therefore, it can be inferred that cathodic wave C1 is ascribed to the bulk electrodeposition of carbon, while the anodic peak A1 is attributed to the oxidation of carbon.

Some researchers considered that the electrochemical reaction of carbonate ions involves an intermediate peroxide ion ( $\text{O}_2^{2-}$ ) [20-21]. Therefore, reaction (5) can be further expressed as follows:



However, there was no obvious signal for peroxide ions during the electrochemical test (Figure 6), which is thought to be due to the instability of peroxide ions on the electrode surface. Peroxide ions can combine with carbon to form  $\text{C-O}_2^{2-}$  and stably exist on the surface of carbon deposited on the electrode [17-18].

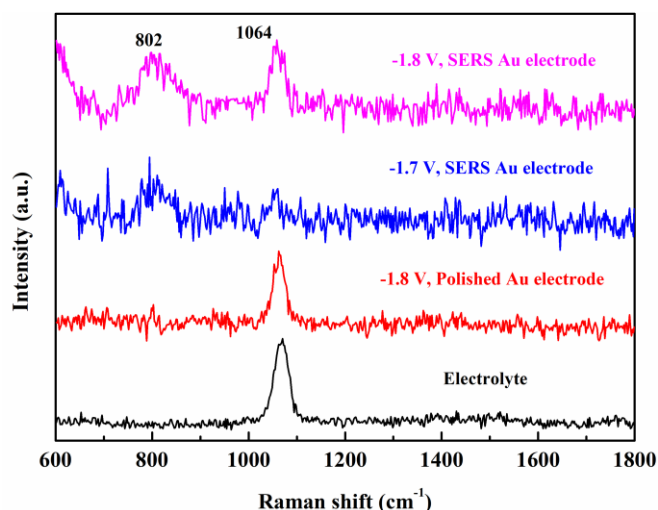


**Figure 8.** In-situ Raman spectra recorded on various electrodes in  $\text{Li}_2\text{CO}_3\text{-K}_2\text{CO}_3$  molten salt during constant potential electrolysis process at 873 K

To explore the presence of peroxide ions ( $\text{O}_2^{2-}$ ) in the reduction process of carbonate ions ( $\text{CO}_3^{2-}$ ), in-situ Raman spectroelectrochemistry experiments were performed on a gold electrode in  $\text{Li}_2\text{CO}_3\text{-K}_2\text{CO}_3$  molten salt. The Raman spectrum recorded on a polished Au electrode during constant potential electrolysis in  $\text{Li}_2\text{CO}_3\text{-K}_2\text{CO}_3$  molten salt at -1.8 V (vs. Pt) is shown in Figure 8. For comparison, the Raman spectrum of the molten salt is also measured. The Raman band appearing at  $1064\text{ cm}^{-1}$  is assigned to the vibration of carbonate. Note that a very weak band is observed at  $802\text{ cm}^{-1}$  in the spectrum of the molten salt, which is attributed to the vibration of peroxide ions ( $\text{O}_2^{2-}$ ) [28-29]. Furthermore, the prepared Au SERS substrate is used as the working electrode to improve the Raman signal in constant potential electrolysis in  $\text{Li}_2\text{CO}_3\text{-K}_2\text{CO}_3$  molten salt. As shown in Fig. 8, an obvious Raman band located at  $802\text{ cm}^{-1}$  is observed when the electrolysis potential is -1.7 V, and the band intensity increases as the potential moves to a more negative value of -1.8 V. This represents an increase in the concentration of peroxide ions in the form of  $\text{C-O}_2^{2-}$  because more carbon is deposited on the Au SERS electrode. The enhanced band is convincing evidence confirming the existence of the intermediate peroxide ions ( $\text{O}_2^{2-}$ ) in the electrochemical reaction of carbonate ion in the form of reactions (7) and (8). This result indicates that the Au SERS substrate prepared by the ORC process can be used to study Raman spectra in high-temperature molten salts.

#### 4. CONCLUSIONS

In this paper, a Au SERS substrate was prepared by a simple oxidation-reduction method and applied to in-situ Raman spectroelectrochemistry to explore the electrochemical reduction reaction mechanism of  $\text{Li}_2\text{CO}_3\text{-K}_2\text{CO}_3$  carbonate molten salt. The main conclusions are as follows:

(1) The Au SERS substrate prepared by the ORC process has a SERS factor of  $1.37 \times 10^4$ , and it presents excellent uniformity and long-term stability.

(2) The Au SERS substrate can withstand attack at high temperatures. After high-temperature treatment at 873 K, it maintains an acceptable SERS factor of  $8.76 \times 10^2$ .

(3) The prepared Au SERS substrate has a certain enhancement effect on the Raman scattering of the complexes in  $\text{Li}_2\text{CO}_3\text{-K}_2\text{CO}_3$  molten salt and the intermediate species in the electrochemical reaction. The existence of the intermediate peroxide ions ( $\text{O}_2^{2-}$ ) during the electrochemical reduction process of carbonate is confirmed.

#### ACKNOWLEDGMENTS

This work was financially supported by the National Natural Science Foundation of China (Grant No. 51974081), and the Natural Science Foundation of Liaoning Province, China (2019-MS-129).

#### References

1. X. Q. Ao, H. Wang and Y. G. Wei, *Chem. Ind. Eng. Pro.*, 26 (2007) 1384.
2. H. J. Wang, S. S. Xu, J. Cheng, R. Y. Zhang, P. J. Wang and Y. Q. Ren, *Ther. Power Genera.*, 46 (2017) 8.
3. W. Weng, L. Tang, and W. Xiao. *J. Energy Chem.*, 28 (2019) 128.
4. Y. Grosu, A. Anagnostopoulos, B. Balakin, J. Krupanek, M. E. Navarro, L. Gonzalez-Fernandez, Y. Ding, and A. Faik. *Sol. Energ. Mat. Sol. C.*, 220 (2021) 110838.
5. B. H. Wang, M. H. Hong, H. J. Wu, M. J. Luo, D. D. Yuan and W. Dong, *Chem. Ind. Eng. Pro.*, 32 (2013) 2120.
6. J. M. Young, A. Mondal, T. A. Barckholtz, G. Kiss, L. Koziol, and A. Z. Panagiotopoulos. *Aiche J.*, 67 (2021) e16988.
7. H. Kawamura and Y. Ito, *J. Appl. Electrochem.*, 30 (2000) 571.
8. Q. S. Song and Q. Xu, *J. Alloy. Compd.*, 647 (2015) 245.
9. M. A. Hughes, R. D. Bennett, J. A. Allen, and S. W. Donne. *RSC Adv.*, 9 (2019) 36771.
10. X. Wang, X. Liu, G. Licht, B. Wang, and S. Licht. *J. CO<sub>2</sub> Util.*, 34 (2019) 303.
11. A. J. Appleby and S. B. Nicholson, *J. Electroanal. Chem. Inter. Electrochem.*, 83 (1977) 309.
12. A. J. Appleby and S. B. Nicholson, *J. Electrochem. Soc.*, 127 (1980) 759.
13. A. J. Appleby and S. B. Nicholson, *J. Electroanal. Chem. Inter. Electrochem.*, 112 (1980) 71.
14. W. M. Vogel and S. W. Smith, *J. Electrochem. Soc.*, 129 (1982) 1668.
15. M. Cassir, G. Moutiers and J. Devynck, *J. Electrochem. Soc.*, 140, (1993) 3114.
16. M. Cassir, B. Malinowska and W. Peelen, *J. Electroanal. Chem.*, 43(1997) 195.
17. K. L. Van and H. Groult, *Electrochim. Acta*, 21 (2009) 4566.
18. A. Borucka, *J. Electrochem. Soc.*, 124 (1977) 972.
19. B. Ren, X. Q. Li, Y. Xie, W. Y. Hu and Z. Q. Tian, *Spectrosc. Spect. Anal.*, 20 (2000) 648.
20. B. Ren and Z. Q. Tian, *Petrochem. Tech.*, 31 (2002) 488.
21. B. Ren and Z. Q. Tian, *Petrochem. Tech.*, 31 (2002) 580.

22. R. M. Katona, R. G. Kelly, C. R. Bryan, R. F. Schaller, and A. W. Knight. *Electrochem. Commun.*, 118 (2020) 106768.
23. A. A. Nekrasov, O. D. Iakobson, and O. L. Gribkova. *Electrochim. Acta*, 290 (2021) 138869.
24. H. Chen, G. C. Jiang, J. L. You and Y. Q. Wu, *Spectrosc. Spect. Anal.*, 27 (2007) 2464.
25. J. Wang, J. L. You, Y. Y. Wang, G. C. Zhang, S. M. Wan, P. Z. Fu, S. T. Yin, Q. Liu, C. Y. Wang and X. W. Liu, *J. Syn. Cry.*, 42 (2013) 397.
26. X. Hu, W. Deng, Z. Shi, Z. Wang, B. Gao, and Z. Wang. *J. Chem. Eng. Data*, 64 (2019) 202.
27. M. Lin, X. Hu, Z. Shi, B. Gao, J. Yu, and Z. Wang. *J. Energy Chem.*, 44 (2020) 19.
28. T. Itoh, K. Abe, K. Dokko, M. Mohamedi, I. Uchida and A. Kasuya, *J. Electrochem. Soc.*, 151 (2004) A2042.
29. T. Itoh, T. Maeda and A. Kasuya, *J. Roy. Soc. Chem.*, 132 (2006) 95.
30. Z. Q. Tian, B. Ren and Z. Q. Wang, *J. Light Scat.*, 10 (1998) 186.
31. B. Ren, J. F. Li, Y. F. Huang, Z. C. Zeng and Z. Q. Tian, *Electrochem.*, 16 (2010) 305.
32. D. Y. Wu, J. F. Li, B. Ren and Z. Q. Tian, *Chem. Soc. Rev.*, 37 (2008) 1025.
33. Z. Q. Tian, B. Ren, J. F. Li and L. Y. Zhi, *Chem. Commun.*, 34 (2007) 3514
34. Z. Q. Tian, B. Ren, and D. Y. Wu. *J. Phys. Chem. B*, 106 (2002) 9463.
35. H. Z. Yu, J. Zhang, H. L. Zhang and Z. F. Liu, *Langmuir*, 15 (1999) 16.
36. L. X. Li, Z. N. Shi, B. L. Gao, J. L. Xu, X. W. Hu and Z. W. Wang, *J. Electrochem. Soc.*, 163 (2016) E1.

© 2021 The Authors. Published by ESG ([www.electrochemsci.org](http://www.electrochemsci.org)). This article is an open access article distributed under the terms and conditions of the Creative Commons Attribution license (<http://creativecommons.org/licenses/by/4.0/>).